Therapeutics, Targets, and Chemical Biology

Cancer Research

Therapeutic Rationale to Target Highly Expressed CDK7 Conferring Poor Outcomes in Triple-Negative Breast Cancer

Bo Li[1], Triona Ni Chonghaile[2], Yue Fan[1], Stephen F. Madden[3], Rut Klinger[1], Aisling E. O'Connor[1], Louise Walsh[4], Gillian O'Hurley[5], Girish Mallya Udupi[5], Jesuchristopher Joseph[5], Finbarr Tarrant[1], Emer Conroy[1], Alexander Gaber[6], Suet-Feung Chin[7], Helen A. Bardwell[7], Elena Provenzano[8], John Crown[9], Thierry Dubois[10], Sabine Linn[11], Karin Jirstrom[6], Carlos Caldas[7], Darran P. O'Connor[4], and William M. Gallagher[1,5]

Abstract

Triple-negative breast cancer (TNBC) patients commonly exhibit poor prognosis and high relapse after treatment, but there remains a lack of biomarkers and effective targeted therapies for this disease. Here, we report evidence highlighting the cell-cycle–related kinase CDK7 as a driver and candidate therapeutic target in TNBC. Using publicly available transcriptomic data from a collated set of TNBC patients ($n = 383$) and the METABRIC TNBC dataset ($n = 217$), we found *CDK7* mRNA levels to be correlated with patient prognosis. High CDK7 protein expression was associated with poor prognosis within the RATHER TNBC cohort ($n = 109$) and the METABRIC TNBC cohort ($n = 203$). The highly specific CDK7 kinase inhibitors, BS-181 and THZ1, each downregulated CDK7-mediated phosphorylation of RNA polymerase II, indicative of transcriptional inhibition, with THZ1 exhibiting 500-fold greater potency than BS-181. Mechanistic investigations revealed that the survival of MDA-MB-231 TNBC cells relied heavily on the BCL-2/BCL-XL signaling axes in cells. Accordingly, we found that combining the BCL-2/BCL-XL inhibitors ABT-263/ABT199 with the CDK7 inhibitor THZ1 synergized in producing growth inhibition and apoptosis of human TNBC cells. Collectively, our results highlight elevated CDK7 expression as a candidate biomarker of poor prognosis in TNBC, and they offer a preclinical proof of concept for combining CDK7 and BCL-2/BCL-XL inhibitors as a mechanism-based therapeutic strategy to improve TNBC treatment. *Cancer Res; 77(14); 3834–45. ©2017 AACR.*

Introduction

Triple-negative breast cancer (TNBC), which is denoted by negative expression of estrogen receptor (ER), progesterone receptor (PR), and HER2, is a heterogeneous subgroup that exhibits substantial genotypic and phenotypic diversity (1, 2). Currently, no established targeted therapeutics or biomarkers of outcome/response have been clinically approved in the context of TNBC. TNBC patients commonly exhibit poor prognosis and high relapse rates at early stages after conventional neoadjuvant chemotherapy treatment (3, 4). The aggressive nature of TNBC is also reflected by an increased likelihood of distant recurrence and death within 5 years following primary intervention (3) and a shorter survival once diagnosed with metastatic disease (5). Interestingly, patients with a pathologic complete response following primary systemic chemotherapy have an excellent 3-year overall survival. In contrast, in patients with residual disease, those with TNBC displayed shorter overall survival (4). This clearly demonstrates that the poorer outcomes observed in TNBC may be largely due to the fraction of patients with chemoresistant disease, which represent over 50% of cases (6). This observation underscores the need to identify the patients that are unlikely to benefit from existing chemotherapeutics using prognostic markers and to develop alternative therapeutic options.

CDK7 belongs to the cyclin-dependent kinase family, a major class of kinases involved in cell-cycle regulation. It binds to cyclin

[1]UCD School of Biomolecular and Biomedical Science, UCD Conway Institute, University College Dublin, Dublin, Ireland. [2]Department of Physiology & Medical Physics, Royal College of Surgeons in Ireland, Dublin, Ireland. [3]Population Health Sciences Division, Royal College of Surgeons in Ireland, Dublin, Ireland. [4]Department of Molecular & Cellular Therapeutics, Royal College of Surgeons in Ireland, Dublin, Ireland. [5]OncoMark Ltd, Belfield Innovation Park, Dublin, Ireland. [6]Lund University, Lund, Sweden. [7]Cancer Research UK Cambridge Institute, University of Cambridge, Li Ka Shing Centre, Cambridge, United Kingdom. [8]Cambridge Experimental Cancer Medicine Centre (ECMR) and NIHR Cambridge Biomedical Research Centre, Cambridge University Hospitals NHS Foundation Trust, Cambridge, United Kingdom. [9]Department of Medical Oncology, St. Vincent's University Hospital, Dublin, Ireland. [10]Institut Curie, PSL Research University, Department of Translational Research, Breast Cancer Biology Group, Paris, France. [11]The Netherlands Cancer Institute, Amsterdam, the Netherlands.

Note: Supplementary data for this article are available at Cancer Research Online (http://cancerres.aacrjournals.org/).

B. Li and T. Ni Chonghaile contributed equally to this article.

D.P. O'Connor and W.M. Gallagher share senior authorship of this article.

Corresponding Author: William Gallagher, UCD School of Bimolecular and Biomedical Science, UCD Conway Institute, University College Dublin, Belfield, Dublin D4, Ireland. Phone: 353-1716-6743; E-mail: william.gallagher@ucd.ie

doi: 10.1158/0008-5472.CAN-16-2546

AACR

H and MAT1 forming a trimeric cyclin-activating kinase (CAK) that executes its function by phosphorylating other CDKs involved in cell-cycle control (7). Each complex controls specific transitions between two subsequent phases in the cell cycle. CDK7 is required for both activation and complex formation of CDK1/cyclin-B during the G_2–M transition and for activation of CDK2/cyclin-E during the G_1–S transition (8). In addition, CDK7 regulates polymerase II–mediated RNA transcription through the binding of CAK to the TFIIH basal transcription factor complex, which phosphorylates the C-terminal domain of the largest subunit of RNA polymerase II (RNAPII) (9, 10). Previously, it was shown that CAK also phosphorylates and enhances activities of transcriptional regulators (11, 12). Therefore, CDK7 affects both cell-cycle progression and transcriptional activity. Recent studies highlighted the role of CDK7 as a transcriptional regulator, a key mechanism that many aggressive cancers rely on, which provided a promising therapeutic target in these hard-to-treat diseases, particularly in TNBC and other cancers that follow MYC-driven oncogenic transcription addiction (13–16).

Numerous attempts have been made to identify key oncogenic pathways altered at the molecular level in TNBC. Previously, a high frequency of mutations in the *TP53* tumor suppressor gene, along with amplification of the transcription factor–encoding *MYC* and the anti-apoptotic *MCL-1* genes, were found in residual neoadjuvant chemotherapy–treated TNBC (17). MYC, a pleiotropic transcription factor that dimerizes with MAX to bind to enhancer box (E-box) sequences in the promoters of active genes, plays a key role in a myriad of tumor types (18). Aberrant expression of MYC family members commonly leads to deregulated transcription and metabolism, resulting in uncontrolled tumor growth and proliferation, and elevated expression of these oncogenes is often linked to poor prognosis (19, 20).

MCL-1 is a member of the antiapoptotic BCL-2 family that governs mitochondrial apoptosis through protein–protein interaction. Given MCL-1 its short half-life, MCL-1 is significantly affected by transcriptional inhibition and is one of the most commonly amplified genes in cancer (21). To date, the small-molecule inhibitors of MCL-1 that have been developed (22) do not have nanomolar affinity of binding equivalent to the BH3 mimetics ABT-263 (binds to BCL-2, BCL-XL and BCL-W; refs. 23–25) and ABT-199 (binds to BCL-2; refs. 26, 27). Inhibition of the antiapoptotic proteins is capable of killing cells that are dependent on those antiapoptotic proteins for survival. BH3 profiling is a useful tool for assessing antiapoptotic dependency. BH3 peptides generated from the functional BH3 domain of particular proapoptotic proteins are added to permeabilized cells and loss of mitochondrial potential or cytochrome *c* is measured as a functional readout of antiapoptotic dependency (28, 29).

Here, we proposed to use an unbiased *in silico* analysis of transcriptomic data to identify kinases whose expression was associated with clinical outcomes in TNBC and validate the findings at the protein level using IHC on tissue microarrays (TMA). From this analysis, expression of CDK7, a cyclin-dependent kinase, was found to be closely associated with poor prognosis at both mRNA and protein levels. Moreover, we evaluated the response *in vitro* to CDK7 inhibition using both short hairpin RNAs (shRNA) and two specific CDK7 inhibitors in TNBC. Inhibition of CDK7 caused inhibition of proliferation, phosphorylation of RNAPII, an indication of transcriptional inhibition, along with induction of apoptosis. MCL-1 and MYC were downregulated in a dose- and time-dependent manner following CDK7 inhibition. Using BH3 profiling, we identified an increased dependency on BCL-2/BCL-XL following CDK7 inhibition and discovered the synergistic combination of the BH3 mimetic ABT-263 with the CDK7 inhibitor THZ1.

Materials and Methods

Study populations

Public TNBC transcriptomic dataset (Cohort I). An *in silico* method was adopted to explore a publicly available TNBC dataset (30) in which a method for assigning TNBC status to transcriptomic data from human breast cancer tissues was employed. A TNBC microarray dataset ($n = 383$) was reanalyzed to identify genes associated with survival, with a particular focus on kinases. TNBC patient samples were defined on the basis of negative mRNA expression of *ER*, *PR*, and *HER2* genes. The TNBC microarray dataset was split into training ($n = 297$) and test ($n = 86$) datasets. The training dataset was used for the discovery study. Univariate Cox regression with proportional hazards models was employed to investigate kinase genes that were significantly associated with patient survival in the training dataset. Candidate survival-associated kinases were then validated in the remaining test dataset. This entire TNBC microarray dataset was derived from patients with a median age of 50 years (range, 28–88 years) at the time of diagnosis, and a median follow-up of 51 months (range, 0–10 years). Patients exhibited tumor grade 1 and grade 2 ($n = 104$) or grade 3 ($n = 234$). Information on tumor grade was missing for 45 patients. Patients were either treated with adjuvant chemotherapy ($n = 259$), or not treated with chemotherapy ($n = 87$). Information on chemotherapy treatment was missing for 37 patients.

Public breast cancer transcriptomic dataset (Cohort II). The online tool, *BreastMark*, was used to identify association between *CDK7* mRNA expression and clinical outcomes in a breast cancer cohort with all subtypes. Information on the *BreastMark* system was previously described (31). In this study, *CDK7* mRNA expression data were analyzed from 2,656 breast cancer patients of mixed subtypes censored at 10 years.

METABRIC breast cancer transcriptomic (Cohort III) and TMA (Cohort V) datasets. The METABRIC study protocol and molecular profiling of the entire cohort were previously described (32). The entire METABRIC transcriptomic dataset consists of 1,992 breast cancer patients. In this study, 1,277 breast cancer patients censored at 10 years were analyzed (Cohort III). TNBC samples were defined by negative mRNA expression of *ER*, *PR* and *HER2* genes ($n = 217$). TNBC patients from this sub-cohort had a median age of 56 years (range, 28–96 years) at the time of diagnosis. The median follow-up was 44 months (range, 0–119 months). Patients were either not treated with any type of therapy ($n = 33$), or treated with chemotherapy, hormonal therapy, radiotherapy, or a combination of these therapies ($n = 184$). Patients exhibited tumor grade 1 ($n = 4$), grade 2 ($n = 24$), or grade 3 ($n = 189$). A total number of 1,992 breast cancer patients, containing mRNA expression data pertaining to CDK7 and MYC, was analyzed for comparison between each subtype of breast cancer in the METABRIC transcriptomic dataset.

The METABRIC TMA cohort (Cohort V) contains 1,286 breast cancer tissues with 218 TNBC cases. In this study, 203 TNBC patient samples censored at 15 years were analyzed. TNBC patients had a median age of 56 years (range, 27–96 years) at

the time of diagnosis. The median follow-up was 62 months (range, 0–176 months). Patients were not treated with any therapy ($n = 29$) or treated with either chemotherapy, hormonal therapy, radiotherapy only, or with combined therapies ($n = 174$). Patients exhibited tumor grade 1 ($n = 2$), grade 2 ($n = 27$), and grade 3 ($n = 171$). Information on tumor grade was missing for 3 patients.

RATHER TMA cohort (Cohort IV). The RATHER TNBC TMA cohort contains tissues from 138 TNBC patients. In this study, 109 TNBC patient samples censored at 15 years were analyzed. These patients were diagnosed between 1986 and 2010 with a median age of 54 years (range, 26–87 years) at the time of diagnosis. The median follow-up was 61 months (range, 1–173 months). Patients were treated with adjuvant chemotherapy ($n = 47$) or not treated with adjuvant chemotherapy ($n = 62$). Patients were treated with radiotherapy ($n = 29$) or not treated with radiotherapy ($n = 80$). Patients exhibited tumor grade 2 ($n = 12$) or grade 3 ($n = 96$). Information on tumor grade was missing for 1 patient.

Consecutive breast cancer TMA cohort (Cohort VI). The consecutive TMA cohort consists of 512 consecutive breast cancer patients diagnosed at the Department of Pathology, Malmo University Hospital, Sweden, during 1988–1992 (33). In this study, a total number of 346 breast cancer patients were censored at 15 years with a median age of 67 years (range, 28–96 years). The median follow-up was 82 months (range, 0–180 months). Patients were not treated with chemotherapy ($n = 247$) or treated with chemotherapy ($n = 20$). Information on chemotherapy was missing for 79 patients.

TCGA breast cancer transcriptomic dataset (Cohort VII). In this study, the The Cancer Genome Atlas (TCGA) breast cancer transcriptomic dataset consisting of 422 breast cancer patients with mixed subtypes was analyzed for *CDK7* and *MYC* mRNA expression in each individual subtype of breast cancer.

Cell culture

All TNBC cell lines were originally purchased from the ATCC in May 2008 and were regularly authenticated by short tandem repeat profiling. The most recent reauthentication was completed in January 2017. BT20 cells were maintained in EMEM medium. BT549, HCC1143, and HCC1937 cells were maintained in RPMI1640 medium. Hs578T and MDA-MB-231 cells were maintained in DMEM medium. All cell culture media were supplemented with 10% FBS, 1% L-glutamine, and 1% penicillin/streptomycin and cells were incubated at 37°C with 5% CO_2. Mycoplasma testing was performed on a monthly basis.

shRNA-mediated knockdown of CDK7

Commercially available (Sigma Aldrich) pLKO vector-based constructs expressing shRNAs targeting CDK7 (CCGGGCTGTAGAAGTGAGTTTGTAACTCGAGTTACAAACTCACTTCTACAGCTTTTT, and CCGGCATTTAAGAGTTTCCCTGGAACTCGAGTTCCAGGGAAACTCTTAAATGTTTTT) or a pLKO.1-puro nonmammalian shRNA control plasmid DNA (CCGGCAACAAGATGAAGAGCACCAACTCGAGTTGGTGCTCTTCATCTTGTTGTTTTT; Sigma Aldrich) were transfected into HEK293 cells using the Genejuice method. Live viruses were collected, filtered, and used to transfect BT549 and MDA-MB-231 cells for 24 hours. Cells were selected using 3 μg/mL puromycin for 5 days.

Colony formation assay

BT549 and MDA-MB-231 transfectants (expressing either non-targeting control shRNA or CDK7 shRNAs) were seeded at 500 cells/well of 6-well plates in 2-mL growth media for 15 days, with media being replaced by fresh growth media every 5 days until colonies were visible. Colonies were stained with crystal violet solution and counted manually.

Wound healing assay

BT549 and MDA-MB-231 transfectants (expressing either non-targeting control shRNA or CDK7 shRNAs) were seeded at 3×10^5 cells per well of 12-well plates in 1-mL growth medium overnight. Growth media were replaced by serum-free media and incubated for 8 hours before scratches were made. Initial pictures were taken immediately after scratches were made and medium was replaced by fresh serum-free media (0 hour time point). Additional pictures were taken at 24 and 48 hours after medium replacement. Analysis was carried out using the T-Scratch software (ETH Zurich) that analyzed the area occupied by cells in the images. Results were graphed as percentage wound closure over time.

Proliferation: MTT cell viability assay

Cell viability was measured using an MTT (3-(4,5-dimethylthiazol-2-yl)-2,5-diphenyltetrazolium bromide) colorimetric assay. BT549 and MDA-MB-231 cells were seeded in sextuplicate at a density of 2,000 cells/well in 96-well plates and were incubated at 37°C in growth media overnight. Cells were treated with various doses of BS-181 and THZ1 for 72 hours. Cells were then incubated with MTT reagent (5 mg/mL) for 3 hours, after which they were solubilized in dimethyl sulfoxide (DMSO). Absorbance was measured using a Wallac 1420 multi-label plate reader at 570 nm. For the combination treatments, cells were seeded at a density of 2,000 cells/well (BT549 and MDA-MB-231), 3,000 cells/well (BT20), and 5,000 cells/well (HCC1937, HCC1143 and Hs578T) in 96-well plates and were incubated at 37°C overnight. Cells were treated for 48 hours simultaneously with THZ1 and ABT-263/ABT-199 at various doses and synergy was measured using the CompuSyn software. Results were normalized to a DMSO-only control and dose–response curves were created using GraphPad Prism.

Immunoblotting

The following antibodies were purchased from Cell Signaling Technology: anti-CDK7 (2916), anti-CDK1 (9116), anti-p-CDK1 (9111), anti-p-RNAPII Ser-2 (8798), anti-p-RNAPII Ser-5 (8807), anti-p-RNAPII Ser-7 (13780), anti-c-MYC (5605), anti-MCL-1 (5453), anti-BCL-2 (2870), and anti-BCL-XL (2764). Antibodies against RNAPII (sc-17798), vinculin (sc-5573), and α-tubulin (sc-5286) were purchased from Santa Cruz Biotechnology. The anti-β-actin (A5316) antibody was obtained from Sigma-Aldrich.

Cell-cycle analysis by flow cytometry

BT549 and MDA-MB-231 cells were collected at 1×10^6 per cell line, washed with PBS and resuspended in PBS (1 mL) per cell line. Prechilled 70% ethanol (2.5 mL) was added to each cell

suspension dropwise while vortexing. Cells were immediately stored at 4°C overnight. Cells were washed with PBS and resuspended in PBS (500 μL) and RNaseA (1 μL of 2.5 mg/mL) was added to each sample and incubated at 37°C for 30 minutes. Propidium iodide (50 μL of 0.5 mg/mL; Sigma P4170) was added to each sample. The BD Accuri C6 plus (BD Biosciences) flow cytometer was subsequently utilized for the cell-cycle analysis.

Immunohistochemistry

Sample slides were deparaffinized and rehydrated using a Leica Autostainer XL. Samples were treated with 1× citrate buffer pH 6.0 at 95°C in the PT module (LabVision, Thermo Fisher Scientific), incubated with 3% H_2O_2, blocked using UV-Block reagent and treated with the anti-CDK7 antibody. Samples were then treated with primary antibody enhancer (PAE), horseradish peroxidase–labeled polymer, DAB, and counterstained with hematoxylin.

Digital slide scanning and automated image analysis

The Aperio ScanScope XT slide scanner (Aperio Technologies) was used for digital scanning at ×20 magnification. ImageScope analysis software was used for viewing and analyzing digital images. Spectrum was used to generate individual tissue spot images for automated analysis. The Nuclear Algorithm (Aperio Technologies) was used to analyze percentage of positive nuclei against total nuclei. Positive intensity was also measured on cell pellet control slides using the Color Deconvolution Algorithm (Aperio Technologies).

Cell death assay: Annexin V/propidium iodide staining

Apoptosis was measured using an Annexin V/propidium iodide assay. Cells were seeded at a density of 3×10^4 (BT549) and 4×10^4 cells/well (MDA-MB-231) in 24-well plates and were incubated at 37°C in growth media overnight. Cells were then treated with various doses of BS-181 and THZ1 for 48 hours or in combination with ABT-263 or ABT-199 for 24 hours. Cells were washed with PBS and resuspended in Annexin binding buffer (10 mmol/L HEPES pH 7.4, 140 mmol/L NaCl, and 2.5 mmol/L CaCl). Cells were then stained with 0.5 mg/mL Annexin V-FITC and 0.5 mg/mL propidium iodide for 15 minutes before analyzing on the BD Accuri 6 plus (BD Biosciences). Results were normalized to a DMSO-only control and dose–response curves were created using GraphPad Prism.

BH3 profiling

The sequence of the BH3-only peptides and method of synthesis used were described previously (34). BH3 profiling was performed by flow cytometry. Briefly, BH3 peptides at 70 μmol/L were incubated with cells that were being gently permeabilized with 0.005% digitonin. Following 60-minute incubation, cells were fixed with 8% formaldehyde for 15 minutes prior to neutralization and staining with cytochrome *c* at 4°C overnight. The loss of cytochrome was measured on a CyAn ADP Analyzer (Beckman Coulter) using the FITC channel. The percentage of peptide-induced mitochondrial depolarization was calculated by normalization to the solvent-only control DMSO (0%).

Study design, implementation, and statistical analysis

Due consideration of REMARK guidelines was given in respect to study design, implementation, and analysis (35). Kaplan–Meier survival analysis was performed using the SPSS statistical analysis software (IBM). The Cox proportional hazard model was used for multivariate analysis to illustrate the relationships between gene/protein expression and breast cancer–specific survival (BCSS), recurrence-free survival (RFS), distant recurrence-free survival (DRFS), and overall survival (OS). Hazard ratios (HR) and 95% confidence intervals (95% CI) were evaluated for each clinicopathologic variable. A two-tailed test with P value < 0.05 was considered to be significant. The CompuSyn method was used to assess synergy of combination drug treatment (36). A combination index value of under 1 was considered to be significant.

Results

High *CDK7* mRNA expression is associated with poor clinical outcomes of patients with TNBC

To identify kinases that are associated with clinical outcomes in TNBC, we reanalyzed publicly available transcriptomic data from a combined cohort of 579 TNBC patients, of which 383 had associated clinical outcome data (Cohort I, public TNBC; ref. 30). From this analysis, *CDK7* mRNA expression was linked to poor prognosis in a TNBC context. Kaplan–Meier survival analysis in Cohort I ($n = 383$) demonstrated that, when a median *CDK7* mRNA expression cut-off point was used for stratification, high *CDK7* mRNA expression was strongly correlated with reduced RFS ($P < 0.001$; HR = 2.152; CI = 1.576–2.939; Supplementary Fig. S1A). Further survival analysis was carried out using *BreastMark*, an online integrated resource to allow evaluation of genes that are associated with survival outcomes in breast cancer and its molecular subtypes, in an unstratified cohort of 2,656 breast cancer patients (Cohort II, *BreastMark*; ref. 31), which demonstrated no significant association between *CDK7* mRNA expression and RFS (Supplementary Fig. S1B), suggesting that *CDK7* is not a prognostic factor in breast cancer as a whole, but rather specifically predicts outcomes in TNBC.

To further validate our findings, we examined *CDK7* mRNA expression in an independent cohort of the METABRIC (Molecular Taxonomy of Breast Cancer International Consortium; Cohort III), which was composed of a discovery set of 997 primary tumors and a validation set of 995 tumors with long-term clinical outcomes (32). Within Cohort III, when a median cut-off point of *CDK7* mRNA expression was used, high *CDK7* mRNA expression was again significantly associated with poor BCSS specifically in the TNBC cohort ($P = 0.023$; HR = 1.598; CI = 1.061–2.406; Supplementary Fig. S1C). We observed no evidence of association between *CDK7* mRNA expression and clinical outcomes when the entire cohort was examined ($P = 0.195$; HR = 0.885; CI = 0.735–1.065; Supplementary Fig. S1D), again indicating that *CDK7* mRNA expression appeared to specifically predict survival outcomes in a TNBC context.

High CDK7 protein expression is associated with poor clinical outcomes in a TNBC context

In silico analysis of transcriptomic data suggested that *CDK7* mRNA level may differentiate TNBC patients with good versus poor outcomes. Here, we attempted to validate these results at the protein level in an independent cohort of patient samples. TNBC tissues obtained from the RATHER consortium (Rational Therapy for Breast Cancer, www.ratherproject.com; Cohort IV, $n = 109$) were immunohistochemically assessed using an optimized anti-CDK7 antibody (Supplementary Fig. S2). Automated image analysis was used to score percentage of tumor nuclei positive for CDK7 protein expression (over total number of tumor cells)

across all samples and was subsequently assessed for associations with clinicopathologic variables. A median cut-off point was chosen in respect of positivity percentage of CDK7, with representative tissue cores illustrating high and low CDK7 protein expression shown in Fig. 1A. Across the RATHER TNBC TMA cohort, a high percentage of CDK7-positive tumor cells was significantly associated with reduced BCSS ($P = 0.012$; HR = 2.516; CI = 1.189–5.324; Fig. 1B), RFS ($P = 0.019$; HR = 2.208; CI = 1.123–4.344; Supplementary Fig. S3A) and DRFS ($P = 0.013$; HR = 2.506; CI = 1.185–5.299; Supplementary Fig. S3C). Multivariate Cox regression analysis demonstrated that CDK7 protein expression and tumor size were independent prognostic factors for reduced BCSS in TNBC (Table 1; for CDK7, $P = 0.006$; HR = 3.045; CI = 1.383–6.701).

Given that we previously observed no correlations between *CDK7 mRNA* expression and outcomes in a noncategorized breast cancer cohort, we subsequently analyzed CDK7 protein expression in tumor tissues from a representative cohort of 346 breast cancer patients comprised of all major subtypes, namely the Consecutive array (Cohort VI; ref. 33), which included 33 TNBC cases. Again, no correlations between CDK7 protein expression and BCSS ($P = 0.313$; HR = 0.794; CI = 0.507−1.245; Fig. 1C), RFS ($P = 0.364$; HR = 0.852; CI = 0.601−1.206; Supplementary Fig. S3B), or DRFS ($P = 0.662$; HR = 0.916; CI = 0.617−1.359; Supplementary Fig. S3D) were found within this cohort, further reinforcing a particular association of CDK7 expression with poor clinical outcomes in patients with TNBC.

To further validate the prognostic value of CDK7 at the protein level in TNBC, we carried out TMA analysis in the METABRIC cohort, which was composed of 203 TNBC tissues plus additional 948 breast cancer tissues from other subtypes. When a median cut-off point was used to stratify low and high expression of CDK7 protein, Kaplan–Meier survival analysis demonstrated a strong negative correlation between CDK7 protein expression and BCSS ($P = 0.007$; HR = 1.921; CI = 1.185–3.113; Fig. 1D), as well as OS ($P = 0.042$; HR = 1.489; CI = 1.011–2.193; Supplementary Fig.

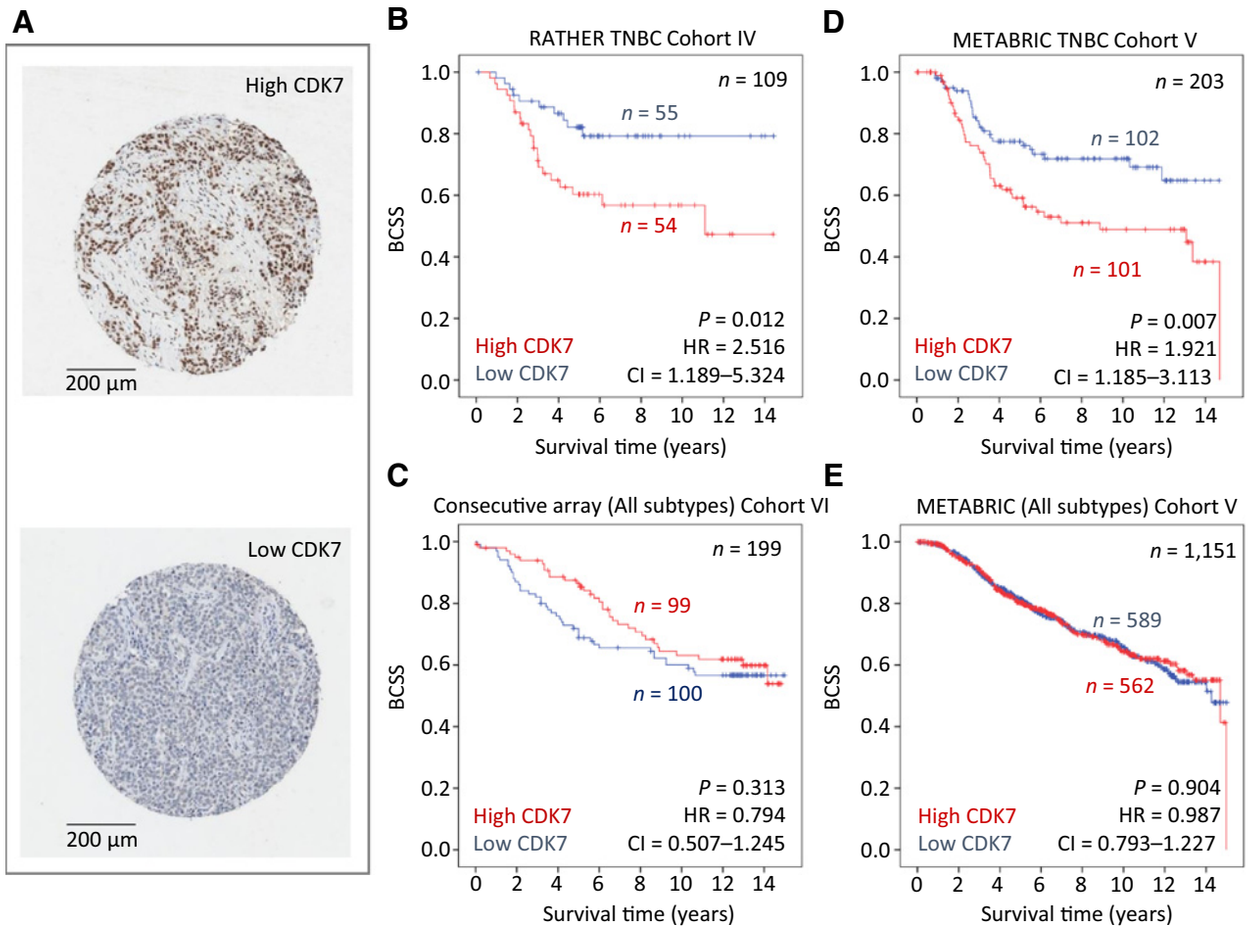

Figure 1.
High CDK7 protein expression is associated with poor prognosis in TNBC tissues. **A,** Representative scanned images of tumor cores with low or high CDK7 protein expression, as determined by IHC. **B,** Kaplan–Meier survival curves showing the relationship between CDK7 protein expression and BCSS in the RATHER TNBC TMA cohort censored at 15 years ($n = 109$). **C,** Kaplan–Meier survival curves showing the relationship between CDK7 protein expression and BCSS in the Consecutive breast cancer TMA cohort censored at 15 years ($n = 199$). **D,** Kaplan–Meier survival curves showing the relationship between CDK7 protein expression and BCSS in the METABRIC TNBC TMA cohort censored at 15 years ($n = 203$). **E,** Kaplan–Meier survival curves showing the relationship between CDK7 protein expression and BCSS in the METABRIC breast cancer TMA cohort censored at 15 years ($n = 1,151$).

Table 1. Multivariate Cox regression analysis of BCSS in the RATHER TNBC dataset

	BCSS	
Clinicopathologic variables	***P***	**HR (95% CI)**
CDK7 protein	0.006	
Low		1
High		3.045 (1.383–6.701)
Age (continuous)	0.427	1.010 (0.985–1.036)
Tumor size (continuous)	0.002	1.397 (1.128–1.730)
Tumor grade	0.802	
Grade 2		1
Grade 3		0.880 (0.323–2.396)
Nodal status	0.675	
No		1
Yes		1.189 (0.530–2.667)
Chemotherapy	0.912	
No		1
Yes		1.044 (0.487–2.237)

S3E), within the TNBC subset of the cohort. Multivariate Cox regression analysis confirmed that CDK7 protein expression and nodal status were independent prognostic factors of reduced BCSS in the TNBC subset (Table 2; for CDK7, $P = 0.003$; HR = 2.136; CI = 1.294–3.526). Similarly, using a median cut-off point, we observed no correlations between CDK7 protein expression and either BCSS ($P = 0.904$; HR = 0.987; CI = 0.793–1.227; Fig. 1E) or OS ($P = 0.168$; HR = 1.122; CI = 0.952–1.322; Supplementary Fig. S3F) across the entire set of METABRIC breast cancer samples. Therefore, we have validated both at the mRNA and at the protein levels that high CDK7 expression is associated with poor prognosis specifically in TNBC.

To further understand the underlying basis of CDK7's association with poor prognosis in TNBC, we compared *CDK7* mRNA expression levels between different subtypes of breast cancer and found that *CDK7* mRNA expression was lower in TNBC compared with luminal A and luminal B subtypes in the METABRIC transcriptomic dataset ($n = 1{,}992$; $P < 0.0001$; Supplementary Fig. S4A) and the TCGA transcriptomic dataset ($n = 422$; $P < 0.0001$; Supplementary Fig. S4B). Previous studies have shown a critical role for CDK7 in mediating superenhancer–linked oncogenic transcription in *MYC*-driven cancer (14) and elevated MYC signaling has been associated with poor prognosis in TNBC (37). Accordingly, we found that *MYC* mRNA expression was higher in TNBC compared with other subtypes of breast cancer in the METABRIC transcriptomic dataset ($P < 0.0001$; Supplementary Fig. S4C), and the TCGA transcriptomic dataset ($P < 0.0001$; Supplementary Fig. S4D).

Table 2. Multivariate Cox regression analysis of BCSS in the METABRIC TNBC dataset

	BCSS	
Clinicopathologic variables	***P***	**HR (95% CI)**
CDK7 protein	0.003	
Low		1
High		2.136 (1.294–3.526)
Age (continuous)	0.254	0.988 (0.967–1.009)
Tumor size (continuous)	0.183	1.008 (0.996–1.020)
Tumor grade	0.131	
Grade 1+2		1
Grade 3		1.957 (0.819–4.676)
Nodal status	0.018	
No		1
Yes		2.446 (1.169–5.117)
Chemotherapy	0.449	
No		1
Yes		0.744 (0.346–1.600)

Knockdown of CDK7 leads to reduced cell proliferation, migration, and increased response to doxorubicin

To investigate the functional impact of CDK7 on TNBC cells, we performed shRNA-mediated knockdown of CDK7 in BT549 and MDA-MB-231 cells. Following efficient knockdown of CDK7 at both mRNA and protein levels detected via RT-PCR and immunoblotting, respectively (Fig. 2A), both BT549 and MDA-MB-231 cell lines with ablated CDK7 demonstrated significantly reduced number of colonies compared with their respective nontargeting controls (Fig. 2B). Cell proliferation was also significantly reduced upon CDK7 knockdown compared with the respective nontargeting controls in both cell lines (Fig. 2C). Moreover, cell migration rate was found dramatically decreased at 24 and 48 hours in cells with CDK7 knockdown (Fig. 2D). Finally, knockdown of CDK7 led to increased TNBC cell sensitivity to doxorubicin following 72 hours of treatment, and only marginally increased responses to carboplatin and no altered response to docetaxel were observed (Fig. 2E), which may be due to a role of CDK7 in the regulation of chemotherapeutic agent–induced DNA damage (38, 39).

Targeting CDK7 with specific inhibitors affects proliferation, apoptosis, and transcription

Recently, a highly specific covalent CDK7 inhibitor THZ1 was developed (13). Here, we compared the efficacy of THZ1 versus a previously discovered noncovalent CDK7 inhibitor BS-181 in the TNBC cell lines BT549 and MDA-MB-231. Cell growth curves demonstrated that both inhibitors reduced cell proliferation in the two cell lines tested (Fig. 3A). Interestingly, the newly developed THZ1 demonstrated an approximately 500-fold higher potency than BS-181 (Fig. 3A). We next assessed whether inhibition of CDK7 caused apoptotic cell death by measuring Annexin V and propidium iodide positivity. Both CDK7 inhibitors induced apoptosis in the BT549 and MDA-MB-231 cell lines (Fig. 3B). Similar to the cell growth curves, THZ1 displayed higher potency in terms of apoptosis induction in comparison with BS-181. Inhibition of CDK7 with THZ1 caused a modest cell-cycle phase redistribution in the MDA-MB-231 cell line, with an approximate increase of 10% of cells in the G_2–M phase (Fig. 3C); a similar trend was observed for BT549 cells but this was not statistically significant. CDK1 is the only essential CDK required for completion of cell mitosis, which is stringently regulated by CDK7 (40). Treatment with THZ1 and BS-181 caused a reduction in phospho-CDK1 in a dose-dependent manner in BT549 and MDA-MB-231 cells (Fig. 3D). In addition, CDK7 plays a key role in RNA transcription regulation by phosphorylating RNAPII (10). Treatment with THZ1 and BS-181 also caused a dose-dependent reduction of phosphorylation of RNAPII at the serine 2, the serine 5 and the serine 7 sites in BT549 and MDA-MB-231 cells (Fig. 3E), suggestive of RNA transcription inhibition through CDK7 inactivation.

The above data demonstrate that CDK7 inhibitors BS-181 and THZ1 trigger antitumor effects by inducing transcription inhibition and apoptosis in a dose-dependent manner.

Combination treatment of THZ1 with ABT-263 shows synergistic effects causing reduced TNBC cell survival

Given the negative effect on RNAPII phosphorylation with CDK7 inhibitor treatment, we assessed the expression of two

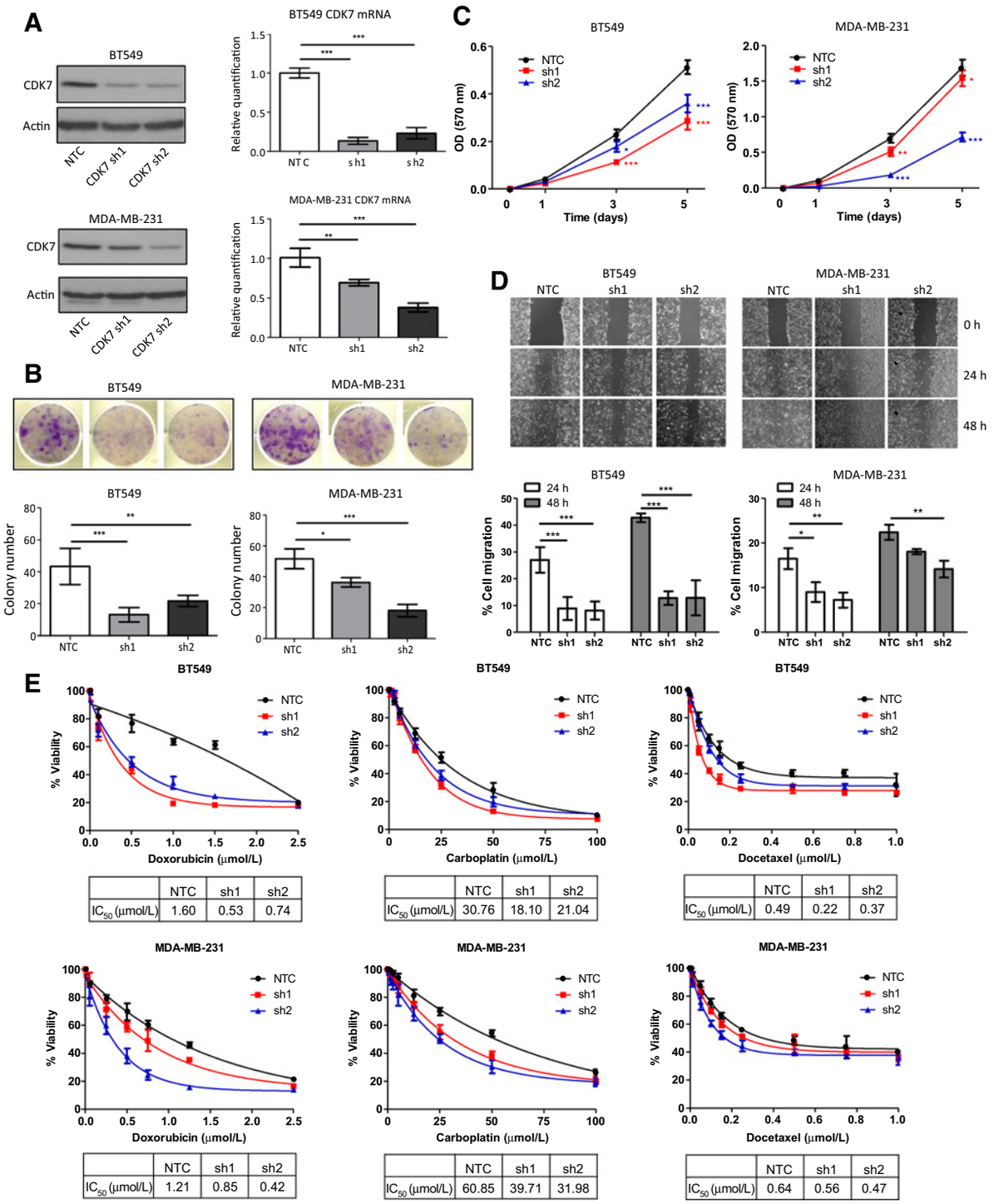

Figure 2.

Knockdown of CDK7 diminishes cell viability, proliferation, migration, and increases cell response to doxorubicin. **A,** Immunoblotting and qRT-PCR analysis of *CDK7* mRNA expression post-shRNA knockdown of CDK7 in BT549 and MDA-MB-231 cells ($n = 3$). A nontargeting shRNA and two independent hairpins targeting CDK7 (shRNA1 and shRNA2) are represented by NTC, sh1, and sh2. Data are presented as mean ± SD (**, $P < 0.01$; ***, $P < 0.001$). **B,** Colony formation assay following CDK7 knockdown in BT549 and MDA-MB-231 cells ($n = 3$). Colony numbers are presented as mean ± SD (*, $P < 0.05$; **, $P < 0.01$; ***, $P < 0.001$). **C,** MTT cell viability assay following CDK7 knockdown in BT549 and MDA-MB-231 cells ($n = 3$). Proliferation is presented as mean absorbance ± SD (**, $P < 0.01$; ***, $P < 0.001$). **D,** Cell migration analysis following CDK7 knockdown ($n = 3$). Migration is presented as mean closure distance ± SD (*, $P < 0.05$; **, $P < 0.01$; ***, $P < 0.001$). **E,** MTT cell viability assay following CDK7 knockdown and treatment with chemotherapeutic agents for 72 hours in BT549 and MDA-MB-231 cells ($n = 3$). IC_{50} values of NTC, shRNA1, and shRNA2 knockdown cells are presented in the mini-tables.

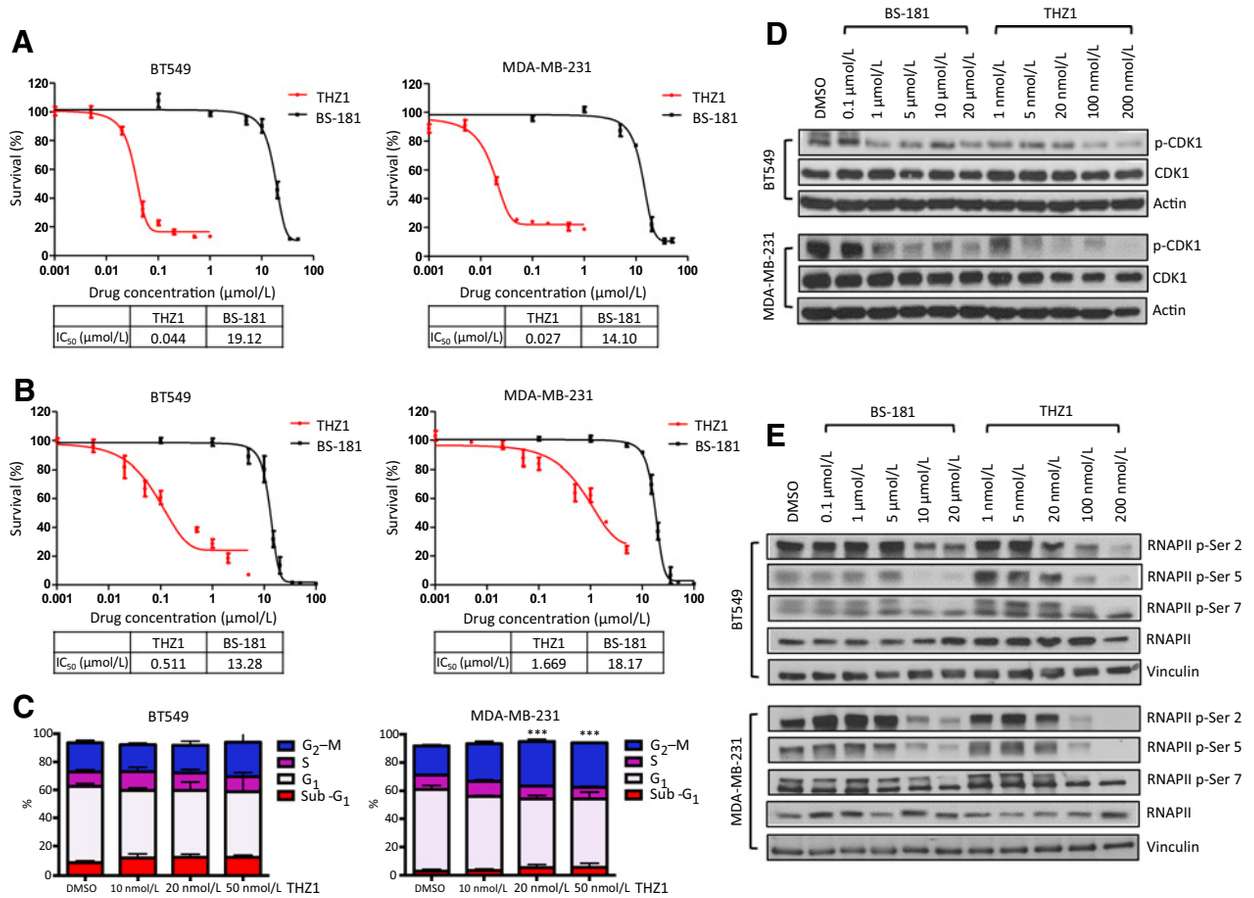

Figure 3.

CDK7 inhibition suppresses cell proliferation and survival via inhibition of RNA transcription. **A,** Cell survival curves showing IC_{50} values of BS-181 and THZ1 in BT549 and MDA-MB-231 cells following 72 hours of treatment. **B,** Apoptosis analysis via Annexin V/propidium iodide staining of BT549 and MDA-MB-231 cells at various concentrations of BS-181 and THZ1 following 48 hours of treatment. **C,** Quantification of percentage of BT549 and MDA-MB-231 cells in different cell-cycle phases following treatment with various doses of THZ1 for 16 hours ($n = 3$; ***, $P < 0.001$). **D,** Immunoblotting of proteins involved in the signaling pathway relating to cell cycle following 4 hours of treatment with various concentrations of BS-181 and THZ1 in BT549 and MDA-MB-231 cells. **E,** Immunoblotting of proteins involved in transcriptional regulation following 4 hours of treatment with various concentrations of BS-181 and THZ1 in BT549 and MDA-MB-231 cells.

proteins with short half-lives, namely the transcription factor c-MYC and the antiapoptotic protein MCL-1. There was a time-dependent reduction in the expression of both c-MYC and MCL-1 following treatment with either BS-181 or THZ1 (Fig. 4A). We assessed the expression of two other antiapoptotic proteins, BCL-2 and BCL-XL, finding that their levels did not alter greatly following exposure to either CDK7 inhibitor (Fig. 4B). Using dynamic BH3 profiling, we aimed to measure the effect of CDK7 inhibition on mitochondrial priming and anti-apoptotic dependency (28, 41). Following treatment for 16 hours with THZ1, BH3 profiling was performed on the MDA-MB-231 cell line. The BH3 peptides BAD and HRK caused a greater loss of cytochrome *c* following treatment with THZ1 (Fig. 4C). The BAD peptide binds to the antiapoptotic proteins BCL-2, BCL-XL and BCL-W, while the HRK peptide only binds to BCL-XL. Following treatment with THZ1, there is a reduction in the expression of MCL-1 (Fig. 4A); therefore, the increased response to the HRK and BAD peptides suggest that pro-death proteins that were bound by MCL-1 now bind to BCL-2/BCL-XL following THZ1 treatment. To test this hypothesis, we combined THZ1 treatment with the BH3 mimetic ABT-263 (which inhibits BCL-2, BCL-XL and BCL-W) in both BT549 (Fig. 4D, I) and MDA-MB-231 (Fig. 4D, II) cell lines. As is evident from the heatmap representation of the MTT assay, the combination treatment caused a synergistic inhibition of proliferation. The combination of THZ1 and ABT-199 caused synergy mainly in the BT549 cell line (Fig. 4D, III), while synergy could not be determined in the MDA-MB-231 cell line as an IC_{50} value for ABT-199 could not be calculated by the MTT assay (Fig. 4D, IV). The combination treatment of THZ1 and ABT-263/ABT-199 was tested in 4 additional TNBC cell lines. MTT assays demonstrated synergistic effects in the HCC1143, HCC1937, and Hs578T cell lines with THZ1 and ABT-263 treatment (Supplementary Fig. S5A). However, the combination treatment of THZ1 and ABT-199 only showed synergy in HCC1937 cells (Supplementary Fig. S5B). No synergy was detected in the BT20

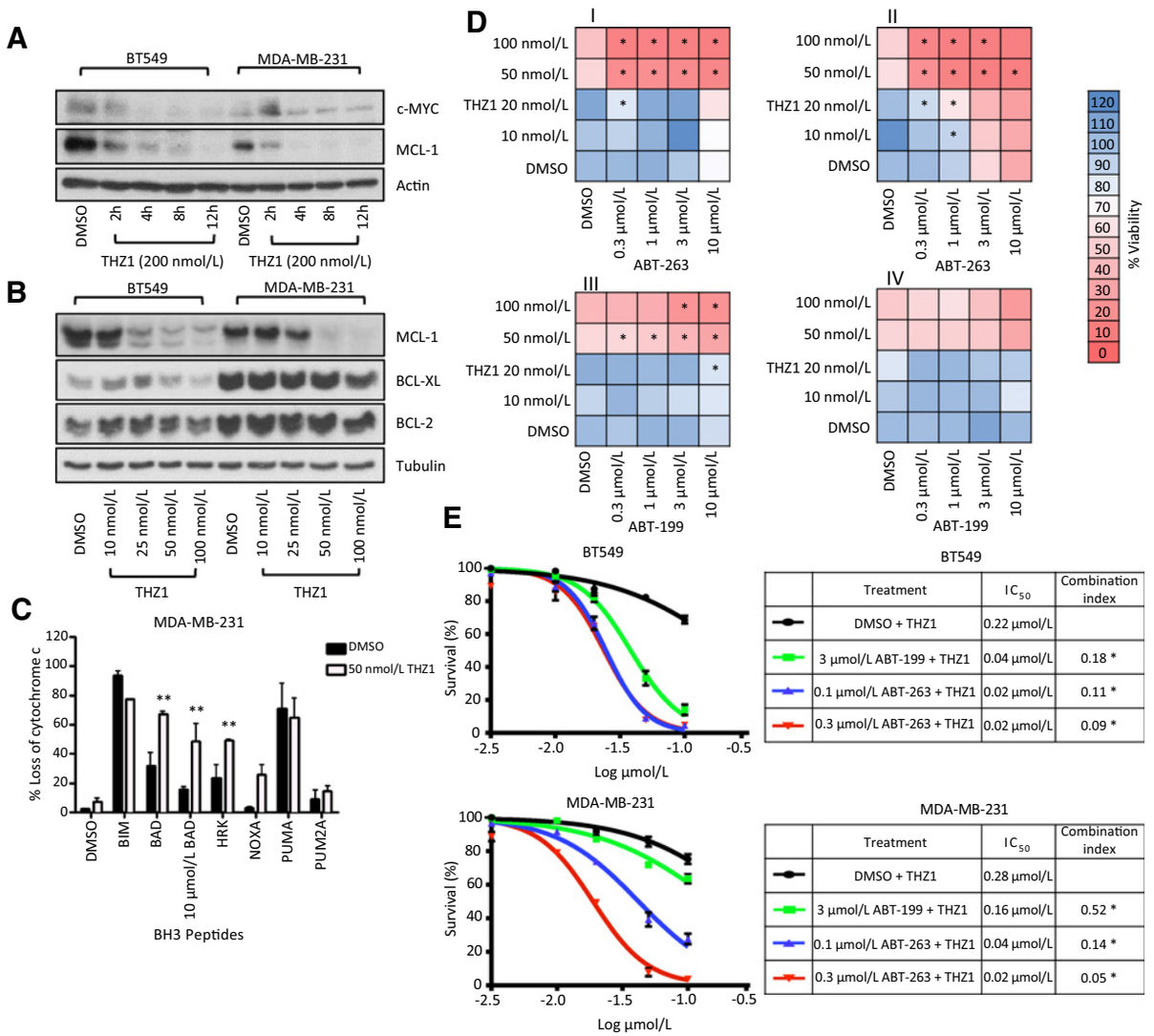

Figure 4.

Identifying rational combination treatments for TNBC. **A,** Immunoblotting of c-MYC and MCL-1 expression following 200 nmol/L THZ1 treatment at increasing time points in BT549 and MDA-MB-231 cells. **B,** Immunoblotting of BCL-2 family protein expression following 24 hours of BS-181 and THZ1 treatment at various concentrations in BT549 and MDA-MB-231 cells. **C,** BH3 profile of MDA-MB-231 cells following treatment with either 50 nmol/L THZ1 or DMSO for 16 hours (**, $P < 0.01$). **D,** MTT viability assay following treatment for 48 hours with escalating concentrations of THZ1 and ABT-263 in BT549 (I) and MDA-MB-231 (II) cells, or treatment with escalating concentrations of ABT-199 and THZ1 in BT549 (III) or MDA-MB-231 (IV) cells. Synergy was calculated using CompuSyn and a combination index value of under 0.7 is marked with an asterisk (*). **E,** Apoptosis analysis via Annexin V/propidium iodide staining on BT549 and MDA-MB-231 cells at various THZ1 concentrations in combination with either DMSO, 0.1 μmol/L ABT-263, 0.3 μmol/L ABT-263, or 3 μmol/L ABT-199 and the combination index was calculated.

cells, suggesting an intrinsically resistant cell line to THZ1 and ABT-263/ABT-199 treatment.

To validate that the combination treatment caused apoptosis and not solely inhibition of proliferation, we assessed the combination using Annexin V and propidium iodide staining. As was evident from the combination index, synergy occurred following combined treatment with THZ1 and ABT-263 at low doses and with ABT-199 at a higher dose in both cell lines (Fig. 4E). Potentially, this suggests that combining the BH3 mimetic ABT-263 may be an effective treatment strategy for TNBC.

Discussion

Limited success has so far been achieved in respect of biomarker identification and validation in TNBC, which may be attributable to disease heterogeneity at the molecular level in this particular subtype. Human proteome studies revealed that more than 50% of human proteins undergo phosphorylation supported by kinases (42), whereas abnormal activation of protein phosphorylation is commonly a cause or consequence of oncogenesis. Kinases have become one of the most intensively pursued classes

of drug targets in cancer. To date, 28 small-molecule kinase inhibitors have been approved by the FDA (43), which has invigorated the search for new kinase inhibitors as anticancer drugs. As such, we focused on discovery of novel kinase biomarkers and tailored therapeutic strategies in TNBC taking advantage of molecular profiling data and preclinical models.

CDK7 has been reported to be a potential therapeutic target in MYC-driven and transcription-dependent cancers (13–16). However, little is known about the value of CDK7 as a prognostic or predictive marker. A recent study revealed that the CAK complex was highly expressed in breast cancer and CDK7 expression was inversely associated with poor prognosis in ER-positive breast cancer, which may be attributable to its role in directly interacting with ERα (44). Our data provided evidence of a negative association between CDK7 expression and survival outcomes specifically in TNBC, together with a potential role in terms of modulating response to chemotherapeutic agents.

Previous reports have linked high expression of p53 (45, 46) and elevated MYC signaling (37) with prognosis in TNBC. However, we found that *MYC* or *TP53* mRNA expression was not significantly correlated with RFS in Cohort I (Public TNBC; Supplementary Fig. S6A and S6B). *MYC* expression showed no association with BCSS in this cohort (Supplementary Fig. S6C), while *TP53* expression was only marginally associated with good BCSS in Cohort III (METABRIC TNBC; Supplementary Fig. S6D). Surprisingly, analysis of *CDK7* mRNA expression in subgroups of breast cancer showed lower overall *CDK7* mRNA expression in the TNBC group compared with the luminal A and luminal B subtypes in Cohort III (METABRIC breast cancer of all subtypes; Supplementary Fig. S4A) and Cohort VII (TCGA; Supplementary Fig. S4B), indicating that CDK7 may be involved in more activities in luminal A and luminal B subtypes compared with TNBC and CDK7′s preferential correlation with poor prognosis in TNBC may be due to its roles in the regulation of transcription and cell cycle. Indeed, CDK7 has previously been shown to mediate ligand-dependent activation of ERα via phosphorylation of serine 118 (11), and the expression of CAK (CDK7, cyclin H, and MAT1) has recently been found to be positively associated with ER expression (44), which correlates with our observation of higher *CDK7* mRNA levels in the luminal A and luminal B subtypes compared with the HER2 and TNBC subtypes (Supplementary Fig. S4A and S4B). Further analysis revealed that *MYC* mRNA expression was higher in TNBC compared with other subtypes (Supplementary Fig. S4C and S4D). Together with the finding that CDK7 inhibition led to reduced MYC expression (Fig. 4A), it is postulated that MYC-dependent TNBC largely relies on the activity of CDK7 during tumor progression.

These findings not only highlight the value of CDK7 as a prognostic marker, but also directly point to therapeutic interventions, such as direct inhibition of CDK7 that could benefit TNBC patients. The dual role of CDK7 in transcriptional regulation and cell-cycle control may offer additional benefits for CDK7-targeted therapy in TNBC. Transcription factors have traditionally been considered "undruggable" targets due to difficulties in directly modulating DNA/protein binding (47). In addition, directly targeting the global transcription machinery may cause intolerable toxicity due to an essential dependency of nontransformed tissue on transcription. Recent studies have challenged the predicament and found that the epigenetic modifier JQ1, a BET bromodomain inhibitor, preferentially inhibits the transcription of genes with superenhancer regions (48). Moreover, TNBC was preferentially sensitive to JQ1 treatment when a broad panel of breast cancer cell lines was assessed (49).

Several studies have been involved in the design and validation of CDK7 inhibitors. BS-181, a highly selective small-molecule CDK7 inhibitor, was found to effectively inhibit the growth of an MCF-7 xenograft (50). Recently, Kwiatkowski and colleagues developed a highly potent covalent CDK7 inhibitor, THZ1, which has been extensively evaluated in various types of cancers and achieved astonishing antiproliferative effects (13–15). A common feature of these tumors is that they appear to be transcriptionally driven. THZ1 preferentially inhibited the proliferation of *MYCN*-driven neuroblastoma and the sensitivity correlated with downregulation of superenhancer-associated genes (14). Similar results were found in small-cell lung cancer with a preferential inhibition of superenhancer-associated genes including *MYC*, *MYCN*, and *OTX2* (15). A recent publication by Wang and colleagues also indicated a preferential sensitivity of TNBC over other breast cancer subtypes to CDK7 inhibition, using a newly developed CDK7 inhibitor THZ2 with improved pharmacokinetic properties (16).

We directly compared, for the first time, the sensitivity of TNBC cell lines to both BS-181 and THZ1 and found that the covalent inhibitor THZ1 was over 500-fold more effective at inhibiting proliferation. Functional assessment of TNBC cells demonstrated that CDK7 downregulation impaired cell viability and proliferation (Fig. 2B and C), indicating that CDK7 plays a key role in the signaling cascades that are responsible for TNBC progression.

At present, chemotherapy is the main systemic treatment option for TNBC patients. Our data suggest a potential role for CDK7 in modulating the sensitivity of TNBC cells to the chemotherapeutic agent doxorubicin (Fig. 2E). This may provide additional therapeutic strategies for the fraction of TNBC patients with poor inherent response to doxorubicin, as well as those displaying residual disease following good initial response to the treatment. We also observed a moderate level of increased sensitivity following CDK7 knockdown with carboplatin treatment, but not with docetaxel treatment (Fig. 2E), suggesting that the apparent protective effect mediated by CDK7 may be limited to genotoxic agents. Previous studies demonstrated that CDK7 played a positive role in DNA damage–induced p53 activation (38, 39). Further investigation of combination treatment with CDK7 inhibitors and chemotherapeutic agents in a broader panel of breast cancer cell lines and *in vivo* is warranted to determine the effectiveness of such combination treatment and potential selectivity/utility in a TNBC context.

Profiling of the residual TNBC tumors following neoadjuvant therapy showed evidence of increased amplification of both *MCL-1* and *MYC* genes (17). Both CDK7 inhibitors, BS-181 and THZ1, inhibited phosphorylation of RNAPII in a dose-dependent manner (Fig. 3E) and caused a reduction in the levels of two short half-life proteins, c-MYC and MCL-1 (Fig. 4A), which point toward the assessment of CDK7 treatment in the refractory setting. Interestingly, the most commonly amplified genes in solid tumors include *MCL-1* and *MYC*, as assessed by somatic copy number alterations in 3,181 different cancer specimens (21). Importantly, MCL-1 has been identified as a crucial survival factor in TNBC and MCL-1 knockdown sensitizes TNBC cell response to BCL-XL inhibition (51).

Using BH3 profiling following treatment with THZ1, we found that the cells became more dependent on the

antiapoptotic proteins, BCL-2 and BCL-XL, as indicated by the increased response to the BAD and HRK BH3 peptides (Fig. 4C). This is likely due to the reduced expression of MCL-1 (Fig. 4B) causing a shift of prodeath proteins to BCL-2/BCL-XL. The BIM and PUMA BH3 peptides did not cause any statistical differences in cytochrome *c* release following THZ1 treatment, indicating that the total expression of prodeath proteins was not altered in response to THZ1. However, a complete dose response of the BIM and PUMA peptides would be required to confirm this. We, therefore, tested the rational combination of THZ1 with the BCL-2/BCL-XL/BCL-W BH3 mimetic ABT-263 or the combination of THZ1 with the BCL-2–specific inhibitor ABT-199.

We found synergy in five out of six triple-negative cell lines treated with ABT-263 and THZ1, demonstrating that the combination shows robust synergy across multiple TNBC cell lines. A recent study showed that the combination of THZ1 and the BH3 mimetic obatoclax was an effective combination treatment for T-cell lymphoma and *in vivo* treatment with the combination did not show any evidence of enhanced toxicity (52). ABT-199 was recently approved by the FDA for the treatment of chronic lymphocytic leukemia with a chromosomal abnormality of 17p deletion. However, we did not detect robust synergy with the BCL-2 specific inhibitor ABT-199 in combination with THZ1, as only two of the six TNBC cell lines tested showed synergy. This suggests that inhibition of both BCL-XL and BCL-2 is necessary in TNBC to robustly detect synergy with THZ1. Taken together, these observations showed evidence of a promising treatment option for TNBC by targeting CDK7 in combination with BH3 mimetics.

In summary, our data demonstrate that CDK7 is associated with poor prognosis in TNBC. Phenotypic changes after kinase depletion indicate that CDK7 is involved in mediating cell proliferation, migration, and doxorubicin-induced DNA damage. Inhibition of transcription using highly specific CDK7 inhibitors has proven here to be promising in targeting TNBC. Furthermore, combined inhibition of CDK7 and BCL-2/BCL-XL using THZ1 and ABT-263 shows synergistic responses, leading to substantial apoptosis. Considering the lack of established targeted therapeutics against TNBC, we propose that CDK7 will be a powerful poor prognostic marker and attractive therapeutic target for TNBC.

Disclosure of Potential Conflicts of Interest

D. O'Connor is a consultant/advisory board member for Pfizer Inc. W.M. Gallagher is a Chief Scientific Officer at OncoMark Limited, reports receiving a commercial research grant from Carrick Therapeutics, and is a consultant/advisory board member for Carrick Therapeutics. No potential conflicts of interest were disclosed by the other authors.

Authors' Contributions

Conception and design: B. Li, T. Ni Chonghaile, C. Caldas, D. O'Connor, W.M. Gallagher

Development of methodology: B. Li, T. Ni Chonghaile, R. Klinger, D. O'Connor

Acquisition of data (provided animals, acquired and managed patients, provided facilities, etc.): T. Ni Chonghaile, L. Walsh, E. Conroy, A. Gaber, S.-F. Chin, E. Provenzano, S.C. Linn, K. Jirstrom, C. Caldas

Analysis and interpretation of data (e.g., statistical analysis, biostatistics, computational analysis): B. Li, T. Ni Chonghaile, Y. Fan, S. Madden, R. Klinger, L. Walsh, G. O'Hurley, G. Mallya Udupi, J. Joseph, F. Tarrant, T. Dubois, D. O'Connor, W.M. Gallagher

Writing, review, and/or revision of the manuscript: B. Li, T. Ni Chonghaile, Y. Fan, R. Klinger, A.E. O'Connor, J. Crown, T. Dubois, S.C. Linn, K. Jirstrom, C. Caldas, D. O'Connor, W.M. Gallagher

Administrative, technical, or material support (i.e., reporting or organizing data, constructing databases): L. Walsh, G. O'Hurley, E. Conroy, A. Gaber, T. Dubois

Study supervision: T. Ni Chonghaile, R. Klinger, A.E. O'Connor, D. O'Connor, W.M. Gallagher

Other (technical histology services): H.A. Bardwell

Acknowledgments

We thank all members of the RATHER consortium, in particular Prof. Rene Bernards from the Netherlands Cancer Institute (Amsterdam, the Netherlands), who provided constructive suggestions for this study. We also thank Dr. Nathanael Gray from the Dana-Farber Cancer Institute (Boston, MA) for the kind gift of the THZ1 inhibitor.

Grant Support

This study was supported by RATHER (Rational Therapy for Breast Cancer), a Collaborative Project funded under the European Union 7th Framework Programme (grant agreement no. 258967), the Irish Cancer Society Collaborative Cancer Research Centre BREAST-PREDICT (CCRC13GAL), and the Science Foundation Ireland Investigator Programme OPTi-PREDICT (grant code 15/IA/3104).

The costs of publication of this article were defrayed in part by the payment of page charges. This article must therefore be hereby marked *advertisement* in accordance with 18 U.S.C. Section 1734 solely to indicate this fact.

Received September 26, 2016; revised March 30, 2017; accepted April 21, 2017; published OnlineFirst April 28, 2017.

References

1. Turner N, Lambros MB, Horlings HM, Pearson A, Sharpe R, Natrajan R, et al. Integrative molecular profiling of triple negative breast cancers identifies amplicon drivers and potential therapeutic targets. Oncogene 2010;29:2013–23.
2. Andre F, Job B, Dessen P, Tordai A, Michiels S, Liedtke C, et al. Molecular characterization of breast cancer with high-resolution oligonucleotide comparative genomic hybridization array. Clin Cancer Res 2009;15:441–51.
3. Dent R, Trudeau M, Pritchard KI, Hanna WM, Kahn HK, Sawka CA, et al. Triple-negative breast cancer: clinical features and patterns of recurrence. Clin Cancer Res 2007;13(15 Pt 1):4429–34.
4. Liedtke C, Mazouni C, Hess KR, Andre F, Tordai A, Mejia JA, et al. Response to neoadjuvant therapy and long-term survival in patients with triple-negative breast cancer. J Clin Oncol 2008;26:1275–81.
5. Harris LN, Broadwater G, Lin NU, Miron A, Schnitt SJ, Cowan D, et al. Molecular subtypes of breast cancer in relation to paclitaxel response and outcomes in women with metastatic disease: results from CALGB 9342. Breast Cancer Res 2006;8:R66.
6. Guarneri V, Broglio K, Kau SW, Cristofanilli M, Buzdar AU, Valero V, et al. Prognostic value of pathologic complete response after primary chemotherapy in relation to hormone receptor status and other factors. J Clin Oncol 2006;24:1037–44.
7. Yankulov KY, Bentley DL. Regulation of CDK7 substrate specificity by MAT1 and TFIIH. EMBO J 1997;16:1638–46.
8. Larochelle S, Pandur J, Fisher RP, Salz HK, Suter B. Cdk7 is essential for mitosis and for in vivo Cdk-activating kinase activity. Genes Dev 1998;12:370–81.
9. Serizawa H, Makela TP, Conaway JW, Conaway RC, Weinberg RA, Young RA. Association of Cdk-activating kinase subunits with transcription factor TFIIH. Nature 1995;374:280–2.
10. Feaver WJ, Svejstrup JQ, Henry NL, Kornberg RD. Relationship of CDK-activating kinase and RNA polymerase II CTD kinase TFIIH/TFIIK. Cell 1994;79:1103–9.
11. Chen D, Riedl T, Washbrook E, Pace PE, Coombes RC, Egly JM, et al. Activation of estrogen receptor alpha by S118 phosphorylation involves a

ligand-dependent interaction with TFIIH and participation of CDK7. Mol Cell 2000;6:127–37.
12. Rochette-Egly C, Adam S, Rossignol M, Egly JM, Chambon P. Stimulation of RAR alpha activation function AF-1 through binding to the general transcription factor TFIIH and phosphorylation by CDK7. Cell 1997; 90:97–107.
13. Kwiatkowski N, Zhang T, Rahl PB, Abraham BJ, Reddy J, Ficarro SB, et al. Targeting transcription regulation in cancer with a covalent CDK7 inhibitor. Nature 2014;511:616–20.
14. Chipumuro E, Marco E, Christensen CL, Kwiatkowski N, Zhang T, Hatheway CM, et al. CDK7 inhibition suppresses super-enhancer-linked oncogenic transcription in MYCN-driven cancer. Cell 2014;159:1126–39.
15. Christensen CL, Kwiatkowski N, Abraham BJ, Carretero J, Al-Shahrour F, Zhang T, et al. Targeting transcriptional addictions in small cell lung cancer with a covalent CDK7 inhibitor. Cancer Cell 2014;26:909–22.
16. Wang Y, Zhang T, Kwiatkowski N, Abraham BJ, Lee TI, Xie S, et al. CDK7-dependent transcriptional addiction in triple-negative breast cancer. Cell 2015;163:174–86.
17. Balko JM, Giltnane JM, Wang K, Schwarz LJ, Young CD, Cook RS, et al. Molecular profiling of the residual disease of triple-negative breast cancers after neoadjuvant chemotherapy identifies actionable therapeutic targets. Cancer Discov 2014;4:232–45.
18. Davis LJ, Halazonetis TD. Both the helix-loop-helix and the leucine zipper motifs of c-Myc contribute to its dimerization specificity with Max. Oncogene 1993;8:125–32.
19. Schwab M, Ellison J, Busch M, Rosenau W, Varmus HE, Bishop JM. Enhanced expression of the human gene N-myc consequent to amplification of DNA may contribute to malignant progression of neuroblastoma. Proc Natl Acad Sci U S A 1984;81:4940–4.
20. Brodeur GM, Seeger RC, Schwab M, Varmus HE, Bishop JM. Amplification of N-myc in untreated human neuroblastomas correlates with advanced disease stage. Science 1984;224:1121–4.
21. Beroukhim R, Mermel CH, Porter D, Wei G, Raychaudhuri S, Donovan J, et al. The landscape of somatic copy-number alteration across human cancers. Nature 2010;463:899–905.
22. Leverson JD, Zhang H, Chen J, Tahir SK, Phillips DC, Xue J, et al. Potent and selective small-molecule MCL-1 inhibitors demonstrate on-target cancer cell killing activity as single agents and in combination with ABT-263 (navitoclax). Cell Death Dis 2015;6:e1590.
23. Wilson WH, O'Connor OA, Czuczman MS, LaCasce AS, Gerecitano JF, Leonard JP, et al. Navitoclax, a targeted high-affinity inhibitor of BCL-2, in lymphoid malignancies: a phase 1 dose-escalation study of safety, pharmacokinetics, pharmacodynamics, and antitumour activity. Lancet Oncol 2010;11:1149–59.
24. Roberts AW, Seymour JF, Brown JR, Wierda WG, Kipps TJ, Khaw SL, et al. Substantial susceptibility of chronic lymphocytic leukemia to BCL2 inhibition: results of a phase I study of navitoclax in patients with relapsed or refractory disease. J Clin Oncol 2012;30:488–96.
25. Gandhi L, Camidge DR, Ribeiro de Oliveira M, Bonomi P, Gandara D, Khaira D, et al. Phase I study of navitoclax (ABT-263), a novel Bcl-2 family inhibitor, in patients with small-cell lung cancer and other solid tumors. J Clin Oncol 2011;29:909–16.
26. Souers AJ, Leverson JD, Boghaert ER, Ackler SL, Catron ND, Chen J, et al. ABT-199, a potent and selective BCL-2 inhibitor, achieves antitumor activity while sparing platelets. Nat Med 2013;19:202–8.
27. Cervantes-Gomez F, Lamothe B, Woyach JA, Wierda WG, Keating MJ, Balakrishnan K, et al. Pharmacological and protein profiling suggests venetoclax (ABT-199) as optimal partner with ibrutinib in chronic lymphocytic leukemia. Clin Cancer Res 2015;21:3705–15.
28. Chonghaile TN, Roderick JE, Glenfield C, Ryan J, Sallan SE, Silverman LB, et al. Maturation stage of T-cell acute lymphoblastic leukemia determines BCL-2 versus BCL-XL dependence and sensitivity to ABT-199. Cancer Discov 2014;4:1074–87.
29. Touzeau C, Ryan J, Guerriero J, Moreau P, Chonghaile TN, Le Gouill S, et al. BH3 profiling identifies heterogeneous dependency on Bcl-2 family members in multiple myeloma and predicts sensitivity to BH3 mimetics. Leukemia 2016;30:761–4.
30. Rody A, Karn T, Liedtke C, Pusztai L, Ruckhaeberle E, Hanker L, et al. A clinically relevant gene signature in triple negative and basal-like breast cancer. Breast Cancer Res 2011;13:R97.
31. Madden SF, Clarke C, Gaule P, Aherne ST, O'Donovan N, Clynes M, et al. BreastMark: an integrated approach to mining publicly available transcriptomic datasets relating to breast cancer outcome. Breast Cancer Res 2013; 15:R52.
32. Curtis C, Shah SP, Chin SF, Turashvili G, Rueda OM, Dunning MJ, et al. The genomic and transcriptomic architecture of 2,000 breast tumours reveals novel subgroups. Nature 2012;486:346–52.
33. O'Brien SL, Fagan A, Fox EJ, Millikan RC, Culhane AC, Brennan DJ, et al. CENP-F expression is associated with poor prognosis and chromosomal instability in patients with primary breast cancer. Int J Cancer 2007; 120:1434–43.
34. Ryan J, Letai A. BH3 profiling in whole cells by fluorimeter or FACS. Methods 2013;61:156–64.
35. McShane LM, Altman DG, Sauerbrei W, Taube SE, Gion M, Clark GM, et al. REporting recommendations for tumor MARKer prognostic studies (REMARK). Nat Clin Pract Urol 2005;2:416–22.
36. Chou TC. Drug combination studies and their synergy quantification using the Chou-Talalay method. Cancer Res 2010;70:440–6.
37. Horiuchi D, Kusdra L, Huskey NE, Chandriani S, Lenburg ME, Gonzalez-Angulo AM, et al. MYC pathway activation in triple-negative breast cancer is synthetic lethal with CDK inhibition. J Exp Med 2012;209:679–96.
38. Ko LJ, Shieh SY, Chen X, Jayaraman L, Tamai K, Taya Y, et al. p53 is phosphorylated by CDK7-cyclin H in a p36MAT1-dependent manner. Mol Cell Biol 1997;17:7220–9.
39. Lu H, Fisher RP, Bailey P, Levine AJ. The CDK7-cycH-p36 complex of transcription factor IIH phosphorylates p53, enhancing its sequence-specific DNA binding activity *invitro*. Mol Cell Biol 1997;17:5923–34.
40. Brown NR, Korolchuk S, Martin MP, Stanley WA, Moukhametzianov R, Noble ME, et al. CDK1 structures reveal conserved and unique features of the essential cell cycle CDK. Nat Commun 2015;6:6769.
41. Ni Chonghaile T, Sarosiek KA, Vo TT, Ryan JA, Tammareddi A, Moore Vdel G, et al. Pretreatment mitochondrial priming correlates with clinical response to cytotoxic chemotherapy. Science 2011;334:1129–33.
42. Wilhelm M, Schlegl J, Hahne H, Moghaddas Gholami A, Lieberenz M, Savitski MM, et al. Mass-spectrometry-based draft of the human proteome. Nature 2014;509:582–7.
43. Wu P, Nielsen TE, Clausen MH. Small-molecule kinase inhibitors: an analysis of FDA-approved drugs. Drug Discov Today 2016;21:5–10.
44. Patel H, Abduljabbar R, Lai CF, Periyasamy M, Harrod A, Gemma C, et al. Expression of CDK7, cyclin H, and MAT1 is elevated in breast cancer and is prognostic in estrogen receptor-positive breast cancer. Clin Cancer Res 2016;22:5929–38.
45. Yamashita H, Nishio M, Toyama T, Sugiura H, Zhang Z, Kobayashi S, et al. Coexistence of HER2 over-expression and p53 protein accumulation is a strong prognostic molecular marker in breast cancer. Breast Cancer Res 2004;6:R24–30.
46. Miller LD, Smeds J, George J, Vega VB, Vergara L, Ploner A, et al. An expression signature for p53 status in human breast cancer predicts mutation status, transcriptional effects, and patient survival. Proc Natl Acad Sci U S A 2005;102:13550–5.
47. Nhili R, Peixoto P, Depauw S, Flajollet S, Dezitter X, Munde MM, et al. Targeting the DNA-binding activity of the human ERG transcription factor using new heterocyclic dithiophene diamidines. Nucleic Acids Res 2013;41:125–38.
48. Loven J, Hoke HA, Lin CY, Lau A, Orlando DA, Vakoc CR, et al. Selective inhibition of tumor oncogenes by disruption of super-enhancers. Cell 2013;153:320–34.
49. Shu S, Lin CY, He HH, Witwicki RM, Tabassum DP, Roberts JM, et al. Response and resistance to BET bromodomain inhibitors in triple-negative breast cancer. Nature 2016;529:413–7.
50. Ali S, Heathcote DA, Kroll SH, Jogalekar AS, Scheiper B, Patel H, et al. The development of a selective cyclin-dependent kinase inhibitor that shows antitumor activity. Cancer Res 2009;69:6208–15.
51. Goodwin CM, Rossanese OW, Olejniczak ET, Fesik SW. Myeloid cell leukemia-1 is an important apoptotic survival factor in triple-negative breast cancer. Cell Death Differ 2015;22:2098–106.
52. Cayrol F, Praditsuktavorn P, Fernando TM, Kwiatkowski N, Marullo R, Calvo-Vidal MN, et al. THZ1 targeting CDK7 suppresses STAT transcriptional activity and sensitizes T-cell lymphomas to BCL2 inhibitors. Nat Commun 2017;8:14290.